

# RESPONSE LATENCY OF VERTEBRATE HAIR CELLS

D. P. COREY AND A. J. HUDSPETH, *Beckman Laboratory of Behavioral Biology,  
Division of Biology 216-76, California Institute of Technology, Pasadena,  
California 91125 U.S.A.*

**ABSTRACT** An in vitro preparation of hair cells from the bullfrog sacculus produces a transepithelial microphonic potential in response to well-defined mechanical stimuli. If corrected for the electrical time constant of the epithelium, the response follows a fast stimulus with a 40- $\mu$ s delay at 22°C. The short latency and its modest temperature dependence limit possible models for transduction by hair cells.

## INTRODUCTION

Because the auditory sensitivity of some animals extends to frequencies as high as 150 kHz (1, 2), it is of interest to know how fast hair cells can transduce stimuli. Recordings of the extracellular microphonic potential from hearing organs of goldfish or cat indicate a response latency of <0.2–0.3 ms (3, 4). However, a more precise measurement of the latency is desirable, especially as it may provide some indication of the nature of the transduction process itself. The rather long latency of vertebrate photoreceptors, for instance, was one of the first indications that a second messenger might be involved in visual transduction (5, 6). In the case of photoreceptors, the ease of presenting temporally well-defined stimuli (light flashes) to the cells facilitates precise measurements of latency. Measurements of latency of response to an acoustic stimulus are complicated, however, by the presence of several mechanical stages between the stimulus and the hair cells. We describe here a system for recording an in vitro microphonic from bullfrog vestibular hair cells while precisely measured mechanical stimuli are presented to the cells, and report a response latency of  $\approx 40 \mu$ s at room temperature.

## METHODS

The sacculi of adult bullfrogs (*Rana catesbeiana*) were dissected from the cartilagenous labyrinths and removed into a dish of saline solution. The region of epithelial tissue surrounding the sensory macula was cut away, and the mass of calcium carbonate crystals (otoconia) was removed. The otolithic membrane, an extracellular matrix that normally couples motion of the mass to the ciliary bundles of the hair cells, remained attached to the bundles (Figs. 1 and 2). The macula was then positioned across a 1-mm hole between two chambers (Fig. 3) so as to separate the chambers ionically and electrically. Chambers were separately perfused with salines similar to those that the cells face in vivo:<sup>1</sup> an artificial endolymph on the apical surface (124 mM K<sup>+</sup>, 5 mM Na<sup>+</sup>, 0.25 mM Ca<sup>++</sup>, 0.11 mM Mg<sup>++</sup>, 130 mM Cl<sup>-</sup>, 3 mM dextrose), and artificial perilymph on the basal surface (3.64 mM K<sup>+</sup>, 122 mM Na<sup>+</sup>, 1.36 mM Ca<sup>++</sup>, 0.68 mM Mg<sup>++</sup>, 130 mM Cl<sup>-</sup>, 3 mM dextrose). No difference was noted, however, when the top chamber instead contained an artificial perilymph. A lightly greased plastic washer was placed over the tissue to secure it and complete the seal. Hair cells were stimulated by moving the otolithic membrane

<sup>1</sup>Maunsell, J. H. R., R. Jacobs, and A. J. Hudspeth. Unpublished observations.

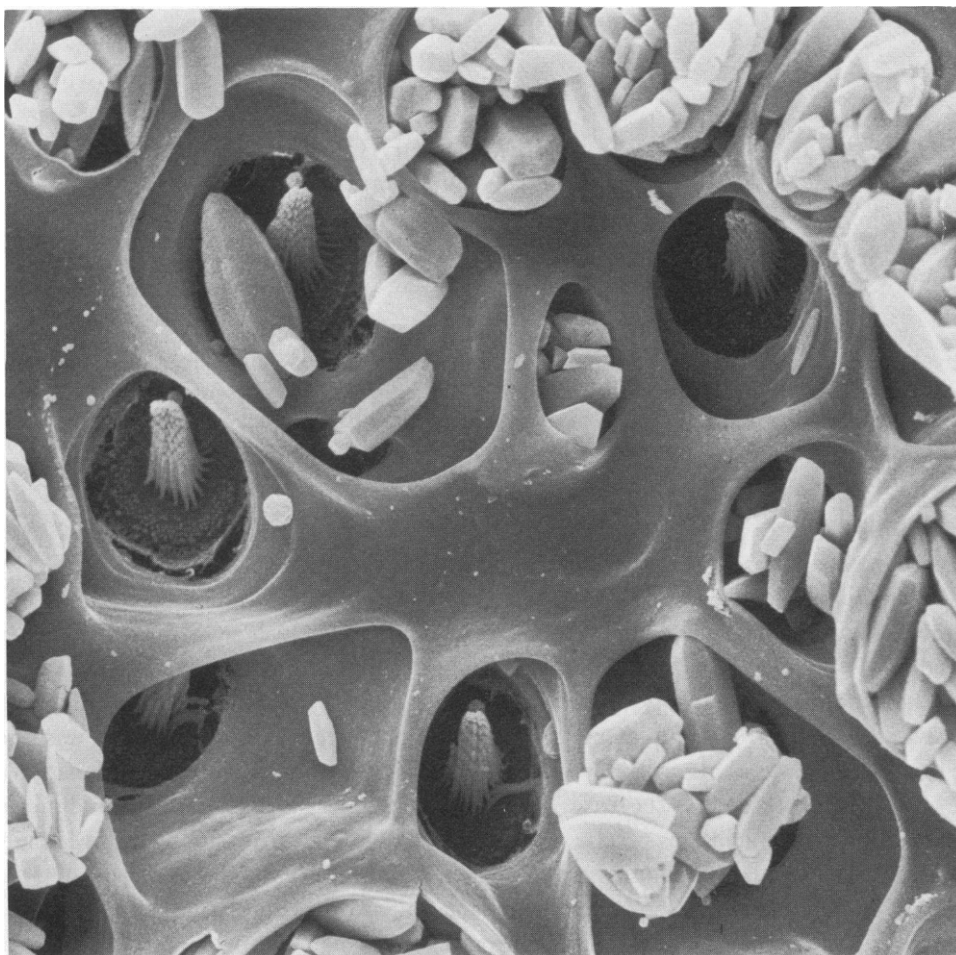


**FIGURE 1** Scanning electron micrograph ( $\times 3,100$ ) of a small region of the sensory macula of the sacculus. Hair bundles protruding from the apical surfaces of the receptor cells insert into holes in the overlying otolithic membrane, some of which retain clusters of otoconia. The preparation, dissected and mounted as for recording, was fixed for 60 min at  $4^{\circ}$  with 40 mM  $\text{OsO}_4$  in 80 mM sodium cacodylate and 10 mM  $\text{CaCl}_2$  at pH 7.3. After dehydration in ethanol, the specimen was critical-point dried and gold sputter-coated.

with a glass probe attached to a piezoelectric bimorph element. The flat bottom of the probe was slightly roughened to engage the membrane. The response was measured by recording the potential between electrodes in the top and bottom chambers (Fig. 4). The differential amplifier used was low-pass filtered at 20 kHz, thereby introducing an 8- $\mu\text{s}$  delay. Data were taken at 5- $\mu\text{s}$  intervals and averaged with a modified PDP 8/E computer (Digital Equipment Corp., Marlboro, Mass.).

## RESULTS AND DISCUSSION

Hair cells are depolarized by displacement of the hair bundle toward the kinocilium (7), a single true cilium which is eccentrically placed in the bundle of stereocilia (modified microvilli), and which thereby defines the orientation of the cell. It is thought that

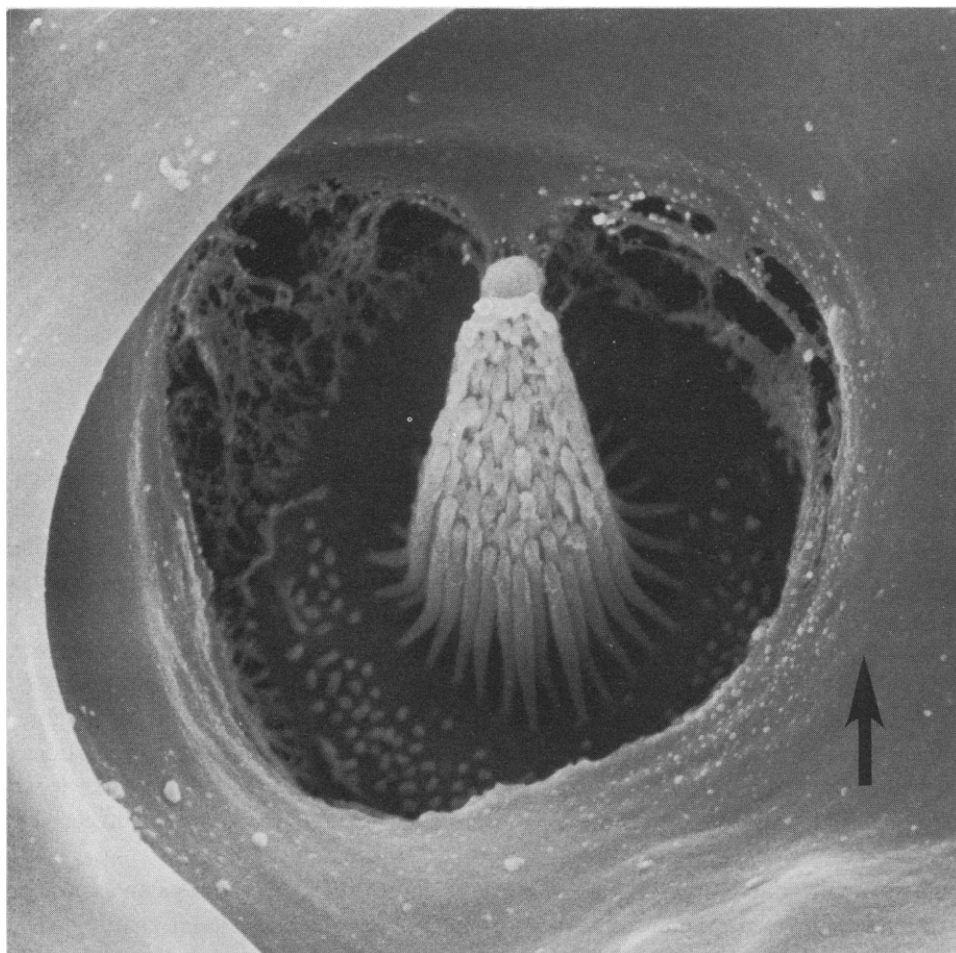


FIGURE 2 The hair bundle of a single hair cell ( $\times 12,300$ ) viewed through a hole in the otolithic membrane. The otolithic membrane has contracted slightly during fixation, revealing the filamentous attachment of the kinociliary bulb to the membrane. Arrow shows the defined orientation.

depolarization is due to an increase in membrane permeability to a cation, an increase specifically at the apical surface of the cell (4, 7–10). As some proportion of the resulting current flow must exit through the basal surface, this would imply a net current through the cell in response to stimulation. The current must flow back across the epithelium to complete the current loop; the resulting microphonic potential would then be the product of the current and the impedance in parallel with the current source, presumably the impedance of the apical surface of the epithelium.

The bulk epithelial impedance was determined by passing known current pulses across the epithelium with a second pair of electrodes and measuring the resulting potential. The distribution of the impedance was found by lowering a glass microelectrode through the epithelium while passing current pulses. Although the potential measured between this electrode and the lower chamber did not change as the electrode traversed the otolithic membrane, the potential dropped abruptly by 90% upon penetration of the apical surface of

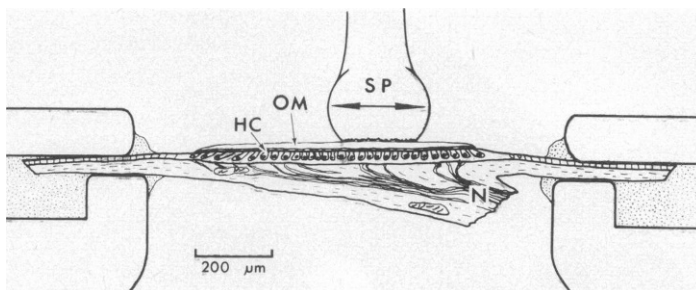


FIGURE 3 The sacculus mounted so as to form a septum between two chambers. Hair cells (HC) and supporting cells form an epithelial sheet. The stimulating probe (SP) contacts the overlying otolithic membrane (OM) to which the hair bundles attach. The saccular branch of the eighth nerve (N) is cut near the macula.

the epithelium. The location of the stimulus-associated current source was determined in addition by mechanically stimulating while lowering the microelectrode. Upon passage of the microelectrode through the apical surface, the evoked microphonic potential wholly disappeared. The stimulus-associated current source and most of the bulk epithelial impedance thus occur in parallel at the apical surface of the epithelium.

In this preparation the impedance is not purely resistive but comprises a capacitance of 35–45 nF in parallel with a resistance of 8–12 k $\Omega$ . These values are similar to those for epithelia, such as frog or *Necturus* gallbladder, with similar tight-junctional morphology (11; unpublished observations). The microphonic potential was thus not directly proportional to the transduction current but was delayed by the capacitance of the epithelium. Knowledge of the epithelial time constant permits one to determine the extent of this delay and to correct for it.

That the *in vitro* microphonic in fact reflects the activity of hair cells rests on a number of observations. If the measured current were associated with an extracellular charge displacement, associated for instance with the otolithic membrane or ciliary bundles, the response should be transient. In fact, the response to a step stimulus was a current maintained over many milliseconds. Addition of the ototoxic antibiotic, streptomycin, or removal of  $\text{Ca}^{++}$  from the apical chamber blocked the response, as it does for the intracellularly recorded receptor potential (7). The waveform of the response was also similar to microphonic potentials measured *in vivo* in other systems (3, 12). As in many other vestibular organs, there are two populations of hair cells in the frog sacculus: cells positioned centrally in the macula—adjacent to the nerve's insertion—are oriented with polarities opposite to those of more peripheral cells. Because the response of hair cells is not linearly proportional to hair

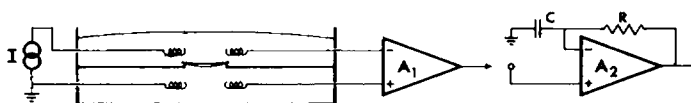


FIGURE 4 Schematic of the recording arrangement. The potential across the epithelium is recorded with a differential amplifier ( $A_1$ ) using Ag/AgCl electrodes. A second pair of electrodes is used to pass current (I) for measuring epithelial impedance. The active filter ( $A_2$ ) can be connected to compensate for the effect of epithelial capacitance.

bundle displacement (7), the summed response had a frequency twice that of the stimulus (13). For these experiments peripheral cells were uncoupled from the stimulus by peeling back the otolithic membrane overlying them (Fig. 5). The response then had the frequency of the stimulus and the polarity appropriate to central cells: displacements toward the kinocilia produced a positive potential in the lower chamber, consistent with a net current from apex to base in hair cells. Stimulation at  $90^\circ$  to the preferred axis elicited little or no response. The response to optimally oriented stimuli was linear for displacements up to  $\approx 0.6 \mu\text{m}$ . As with microphonics recorded in vivo and receptor potentials recorded intracellularly, the response saturated with larger displacements, reaching a plateau more rapidly for displacements away from the kinocilium than for those toward it (3, 7, 13). The total operating range of the aggregate of  $\approx 1,000$  central cells was  $\approx 1.5 \mu\text{m}$ , somewhat larger than the range measured with intracellular recording from single cells.

For the experiments described here, central cells were stimulated with a fast pulse  $0.5 \mu\text{m}$  in amplitude and  $150 \mu\text{s}$  in duration; experiments using step stimuli gave comparable results. The motion of the stimulus probe was measured by positioning it so as partly to occlude a beam of light striking a photodiode. Lateral motion of the probe thus produced a change in photocurrent, which was converted to voltage and amplified. This optical monitor has a resolution of  $0.01 \mu\text{m}$ ; its  $7\text{-}\mu\text{s}$  response time matches that of the microphonic recording system.

The same device was used to measure coupling between the probe and the otolithic membrane. The preparation was viewed with a compound microscope, and an image of the field projected onto a screen. Scattered clumps of otoconia,  $10\text{--}20 \mu\text{m}$  across, remain embedded in the otolithic membrane after removal of the otoconial mass (Fig. 1). Individual clumps could be used to occlude light striking the photodiode; they thus served as markers for otolithic membrane motion.

Regions of the membrane immediately adjacent to the stimulus probe were found to follow the probe displacement with no detectable latency. The stimulus propagated to more distal

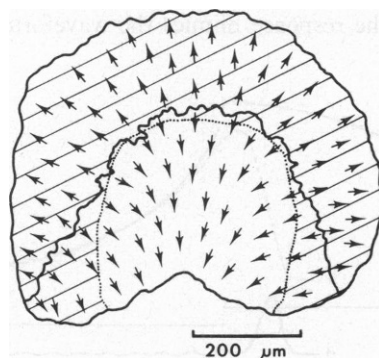


FIGURE 5 Map of orientations for the several thousand hair cells in the macula, obtained from scanning electron microscopy of several preparations. The solid line indicates the point of reversal of orientation (the "striola"). For recordings, the otolithic membrane was peeled off hair cells in the shaded peripheral region, leaving coupled a largely homogeneous group of central cells. The stimulus probe was placed in the middle of this area.

regions with a conduction velocity of  $6.5 \pm 1.1 \mu\text{m}/\mu\text{s}$  (SD), reaching the limit of the central, responsive region in  $\approx 15 \mu\text{s}$ . Over the whole of the responsive region, however, the average delay was  $4.7 \mu\text{s}$ , and is considered negligible for these experiments. It remains an assumption that each hair bundle follows the motion of the overlying otolithic membrane without significant delay.

The electrical response to a pulse stimulus had a rapid rising phase and an exponential decay. One such response is shown in Fig. 6; the decay phase had a time constant of  $370 \mu\text{s}$ . In comparison, external current passed across the membrane produced a typical exponential charging curve, also with a time constant of  $370 \mu\text{s}$ . This similarity in time-course adds considerable support to the contention that the microphonic potential is generated by the net transduction current through the hair cells passing back across the bulk epithelial impedance. It implies also that the shape of the response is largely determined by the passive electrical properties of the epithelium, and thus that the response to a fast mechanical pulse is a fast current pulse convoluted by the low-pass RC filter characteristics of the epithelium.

The effects of epithelial capacitance may, in general, be eliminated by voltage clamping the epithelium. The series access resistance of the chamber ( $\approx 1.5 \text{ k}\Omega$ ), however, limits the response time of a clamp to  $\approx 50 \mu\text{s}$ . Instead, the recorded microphonic potential was corrected by a simple active filter (an augmenting differentiator; transfer function  $V_0 = V_i + \tau dV_i/dt$ ) which performs the inverse operation of a first-order low-pass filter. Square current pulses were passed across the epithelium and its time constant determined from the charging curve by measuring directly from the oscilloscope screen or by electronically taking the logarithm of the curve and measuring the slope. Separate measurements of the time constant were usually equal within 4%. When the active filter was set to the measured time constant, the corrected charging curve showed a square waveform, a further check on the measurement of the time constant. In fact, the measured latency is fairly insensitive to the choice of time constant for the active filter: a 25% change in  $\tau$  changes the apparent latency by  $< 5 \mu\text{s}$ . The filter itself introduced a delay of  $4 \mu\text{s}$ .

The microphonic potential, corrected by the active filter, then reflects the time-course of the transduction current and thus the stimulus-associated conductance change in hair cells (Fig. 7). It can be seen that the response mimics the waveform of the stimulus, with some

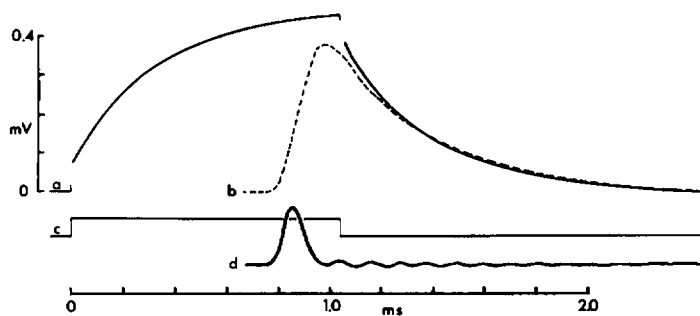


FIGURE 6 Comparison of the waveform of the charging curve (a) generated by passage of a 40-nA current step (c), and the response (b) to a fast mechanical stimulus (d) of  $0.5 \mu\text{m}$  amplitude. The time constant of both the charging curve and the decay phase of the response is  $370 \mu\text{s}$ ; the charging curve shows, in addition to the exponential charging, a step due to the series access resistance of the chamber.

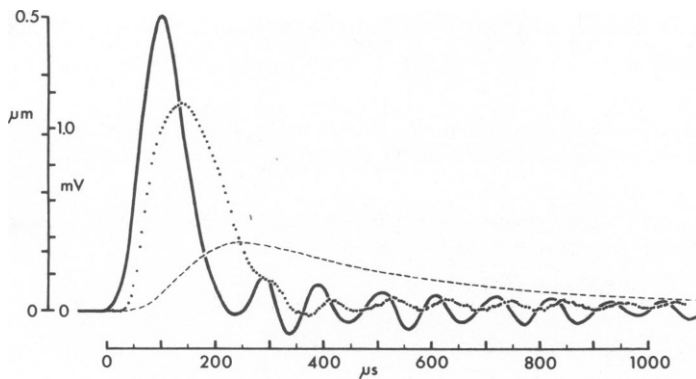


FIGURE 7 Response latency with active filter correction. The probe motion (heavy line) is a pulse 150  $\mu$ s in duration and 0.5  $\mu$ m in amplitude, with some ringing after the pulse. The dashed line is the uncorrected response from Fig. 6. The corrected response (dotted line) mimics in form and follows closely after the probe motion. The magnitude of the probe motion is scaled for this figure by matching the steady-state response to a step with the amplitude of the step.

broadening and with a delay of  $\approx 40 \mu$ s ( $40 \pm 5$  SD,  $n = 9$ ,  $22^\circ\text{C}$ ). This delay is nearly two orders of magnitude less than that measured for vertebrate photoreceptors (14) and by itself places some constraints on possible models for transduction. 40  $\mu$ s, for instance, permits ionic diffusion over a distance of no more than 0.5  $\mu$ m, assuming three-dimensional diffusion of an ion with diffusion constant  $D = 1.3 \times 10^{-5} \text{ cm}^2/\text{s}$ , as for  $\text{K}^+$  in squid axoplasm (15). If a second messenger is involved in hair cell transduction, the last mechanical stage must be physically close to the ionic conductance element.

In addition, the latency increased only moderately as the temperature was lowered. Over the range from  $38$  to  $1^\circ\text{C}$ , the  $Q_{10}$  had a value of  $\approx 2.5$ . This is more than that expected for a diffusion process ( $Q_{10} \approx 1.2$ ), so it is unlikely that diffusion accounts for much of the delay. On the other hand, the moderate temperature dependence and short delay argue against mechanisms of great complexity, such as those involving phosphorylation of membrane proteins (16, 17). We have assumed that the hair bundle follows exactly the displacement of the otolithic membrane. This may not be true: mechanical relaxation of the bundle to the displaced position may contribute to the delay.

Perhaps the most likely mechanism for the rate-limiting step involves transition kinetics of a conductance element. Both the magnitude of the delay and its temperature dependence are similar to those of gating of  $\text{Na}^+$  channels in nerve (18, 19), or acetylcholine receptor channels at the motor endplate (20, 21). Thus the response latency may reflect the gating kinetics of stimulus-activated conductance channels in the hair cell membrane. The measured current is not itself a gating current: its magnitude is much larger than that predicted for a reasonable gating current and it vanishes when permeant ions are removed.

There remains uncertainty as to whether these results may be extended to all vertebrate hair cells, particularly those of the mammalian cochlea. The latency of frog saccular hair cells is just 13  $\mu$ s at  $37^\circ\text{C}$ . From measurements of round window velocity and cochlear microphonic phase at the first turn of the guinea pig cochlea, it is possible to estimate a lag of 50  $\mu$ s (4) to 70  $\mu$ s (22). Correction of these data for tissue capacitance and basilar membrane travel time might yield a still shorter value for the actual latency of mammalian cochlear hair cells. It

thus appears that hair cells of widely varied origin and function share a transduction process of remarkable speed.

We thank R. A. Jacobs for scanning electron microscopy and J. H. R. Maunsell and K. J. Fryxell for developing the computer system. We also appreciate comments on the manuscript from them and from D. C. Van Essen and J. L. Bixby.

This work was supported by National Institutes of Health grants NS-13154 and GM-07616, and by the Ann Peppers, William Randolph Hearst, and Alfred P. Sloan Foundations.

Received for publication 14 December 1978.

## REFERENCES

1. GRINNELL, A. D. 1963. The neurophysiology of audition in bats: intensity and frequency parameters. *J. Physiol. (Lond.)* **167**:38–66.
2. SALES, G., and D. PYE. 1974. Ultrasonic Communication by Animals. Chapman & Hall Ltd., London.
3. FURUKAWA, T., and Y. ISHII. 1967. Neurophysiological studies on hearing in goldfish. *J. Neurophysiol.* **30**:1377–1403.
4. DALLOS, P. 1973. The Auditory Periphery. Academic Press Inc., New York.
5. HAGINS, W. A. 1972. The visual process: excitatory mechanisms in the primary receptor cells. *Ann. Rev. Biophys. Bioeng.* **1**:131–158.
6. PENN, R. D., and W. A. HAGINS. 1972. Kinetics of the photocurrent of retinal rods. *Biophys. J.* **12**:1073–1094.
7. HUDSPETH, A. J., and D. P. COREY. 1977. Sensitivity, polarity, and conductance change in the response of vertebrate hair cells to controlled mechanical stimuli. *Proc. Natl. Acad. Sci. U.S.A.*, **74**:2407–2411.
8. DAVIS, H. A. 1965. A model for transducer action in the cochlea. *Cold Spring Harbor Symp. Quant. Biol.* **30**:181–190.
9. HONRUBIA, V., D. STRELIOFF, and S. T. SITKO. 1976. Physiological basis of cochlear transduction and sensitivity. *Ann. Otol. Rhinol. Laryngol.* **85**:697–711.
10. FURUKAWA, T., Y. ISHII, and S. MATSUURA. 1972. An analysis of microphonic potentials of the sacculus of goldfish. *Jpn. J. Physiol.* **22**:603–616.
11. CLAUDE, P., and D. A. GOODENOUGH. 1973. Fracture faces of zonulae occludentes from “tight” and “leaky” epithelia. *J. Cell. Biol.* **58**:390–400.
12. FLOCK, Å. 1965. Electron microscopic and electrophysiological studies on the lateral line organ. *Acta Oto-laryngol. Suppl.* **199**:1–90.
13. FLOCK, Å., and J. WERSÄLL. 1962. A study of the orientation of the sensory hairs of the receptor cells in the lateral line organ of fish, with special reference to the function of the receptors. *J. Cell Biol.* **15**:19–27.
14. BROWN, K. T., and M. MURAKAMI. 1964. A new receptor potential of the monkey retina with no detectable latency. *Nature (Lond.)* **201**:626–628.
15. HODGKIN, A. L., and R. D. KEYNES. 1953. The mobility and diffusion coefficient of potassium in giant axons from *Sepia*. *J. Physiol. (Lond.)* **119**:513–528.
16. GREENGARD, P. 1976. Possible role for cyclic nucleotides and phosphorylated membrane proteins in postsynaptic actions of neurotransmitters. *Nature (Lond.)* **260**:101–108.
17. HARTZELL, H. C., S. W. KUFFLER, R. STICKGOLD, and D. YOSHIKAMI. 1977. Synaptic excitation and inhibition resulting from direct action of acetylcholine on two types of chemoreceptors on individual amphibian parasympathetic neurones. *J. Physiol. (Lond.)* **271**:817–846.
18. HODGKIN, A. L., and A. F. HUXLEY. 1952. A quantitative description of membrane current and its application to conduction and excitation in nerve. *J. Physiol. (Lond.)* **117**:500–544.
19. FRANKENHAEUSER, B., and L. E. MOORE. 1963. The effect of temperature on the sodium and potassium permeability changes in myelinated nerve fibers of *Xenopus laevis*. *J. Physiol. (Lond.)* **169**:431–437.
20. ANDERSON, C. R., and C. F. STEVENS. 1973. Voltage clamp analysis of acetylcholine produced end-plate current fluctuations at frog neuromuscular junction. *J. Physiol. (Lond.)* **235**:655–691.
21. LESTER, H. A., M. M. NASS, M. E. KROUSE, N. H. WASSERMAN, and B. F. ERLANGER. 1978. ACh receptor-channels begin to open within 30  $\mu$ sec after agonist is applied. *Soc. Neurosci. Abstr.* **4**:370. (Abstr.)
22. TASAKI, I., H. DAVIS, and J.-P. LEGOUX. 1952. The space-time pattern of cochlear microphonics (guinea pig), as recorded by differential electrodes. *J. Acoust. Soc. Am.* **24**:502–519.